Influence of Microstructure and Hydrogen Solubility on the Creep Behavior of Zircaloy-4 and HANA-6 Cladding

Sungjun Choi, Ho-A Kim, Sangtae Kim*
Department of Nuclear Engineering, Hanyang University, 222 Wangsimni-ro, Seongdong-gu, Seoul, 04763 Republic of Korea
*Corresponding author: sangtaekim@hanyang.ac.kr

***Keywords :** creep, zirconium hydride, spent nuclear fuel cladding, electron backscatter diffraction

1. Introduction

Spent nuclear fuel (SNF) undergoes vacuum drying before dry storage, where cladding is exposed to high temperature and pressure from helium and fission products. These conditions can cause creep, a time-dependent deformation under stress. Understanding creep in hydrogen-charged cladding is critical for the integrity and safety of SNF storage [1–4].

This study examines the creep response of low-burnup Zircaloy-4 cladding with typical hydrogen contents, considering the effect of recrystallization. For comparison, HANA-6 cladding with inherently larger grains from its fabrication history was also tested. This allows analysis of how microstructure and hydrogen concentration jointly influence creep.

The systematic approach offers insight into cladding degradation mechanisms. The results will improve evaluation and modeling of creep under dry storage, ultimately supporting long-term safety and reliability of nuclear fuel management.

2. Methods and Results

2.1 Material preparation

Cold-worked stress-relieved (CWSR) Zircaloy-4 cladding tubes, with an outer diameter of 9.5 mm, a thickness of 0.57 mm, and a gauge length of 4 mm, were used in this study. To obtain specimens with different microstructures and grain sizes, ring-shaped samples underwent annealing in a Sieverts apparatus.

2.2 Electron backscatter diffraction (EBSD) analysis

Zircaloy-4 specimens were prepared for EBSD analysis mechanical polish with abrasive papers. The surfaces were further polished using Lectropol-5 electro-polisher at –25°C, applying a voltage of 35 V for 25 seconds in a solution containing 5% perchloric acid and methanol. EBSD data were collected using a JSM-IT800 scanning electron microscope at an acceleration voltage of 20 kV and a magnification of 1000x on the normal direction-transverse direction (ND-TD) cross-sectional plane of the ring specimens.

2.3 Creep test

Creep strain was monitored using a linear variable differential transformer (LVDT) positioned at the center of the testing apparatus, which was directly connected to the main controller. For ring-shaped specimens, a custom-designed semi-cylindrical fixture was employed in place of a conventional dog-bone specimen holder. Prior to mounting the ring specimens, a thin layer of lubricant was applied to the contact surfaces to reduce friction and ensure a uniform stress distribution. Temperature was measured and regulated through an integrated system equipped with K-type thermocouples. The testing procedure began with heating the specimen to 450 °C at a controlled rate of 5 °C/min, followed by a stabilization period of 1 hour. After thermal stabilization, a load of 27.9 kg, corresponding to an applied stress of 120 MPa, was imposed.

2.4 Results

To obtain a range of average grain sizes, the heat treatment temperature and time were varied. In Figure 1, for the Zircaloy-4 cladding, the average grain size in the as-received state was 1.19 μm, and when annealed at 500°C, the grain size increased with increasing time. It reached 1.63 μm after 2 hours, 1.97 μm after 6 hours, 2.6 μm after 12 hours, and 3.12 μm after 24 hours. When annealed at 700°C for 24 hours, it increased to 5.59 μm, showing that the heat treatment temperature and time affect grain growth. In contrast, in Figure 2, the average grain size of the HANA-6 cladding showed almost no change. The grain size in the as-received state was 2.15 μm, and only a slight increase to 2.3 μm was observed after heat treatment at 500°C for 24 hours, demonstrating resistance to grain growth under the same conditions.

Figure 3 shows that the effect of hydrogen concentration on creep behavior varied depending on the average grain size. In the CWSR specimen with an average grain size of 1.19 μm, the secondary creep rate decreased and the creep rupture time increased as the hydrogen concentration increased. A similar trend was observed in the 500°C, 6-hour annealed specimen with an average grain size of 1.97 μm, with the secondary

creep rate decreasing and the creep rupture time increasing as the hydrogen concentration increased.

However, a different trend was observed in the 500°C, 12-hour annealed specimen with an average grain size of 2.6 μm. The secondary creep rate increased and the creep rupture time shortened as the hydrogen concentration approached the TSSD. However, as the hydrogen concentration increased beyond the TSSD, the secondary creep rate decreased and the creep rupture time increased. At this stage, the hydrogenated specimens fractured faster than the unhydrogenated specimens, and especially from the hydrogen concentration of 691 wppm, they fractured more slowly than the unhydrogenated specimens.

A similar trend was observed in the specimens heat-treated at 700°C for 24 hours with an average grain size of 5.59 μm. As the hydrogen concentration approached the TSSD, the secondary creep rate increased and the creep rupture time shortened. However, when the hydrogen concentration exceeded the TSSD, the secondary creep rate decreased and the creep rupture time increased. Furthermore, the hydrogenated specimens fractured much faster than the unhydrogenated specimens.

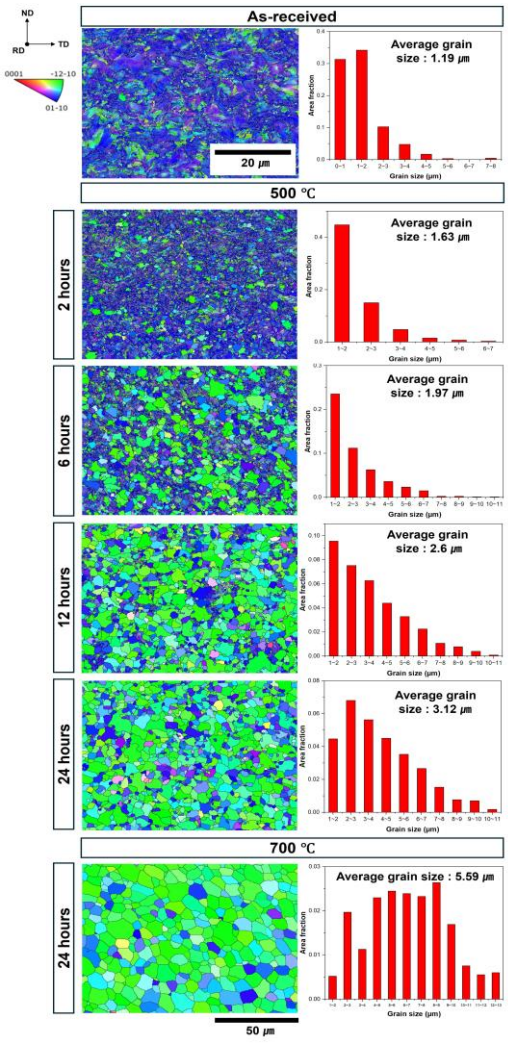

Fig. 1. IPF maps and grain size area fraction plots of Zircaloy-4 in the as-received condition and after heat treatments at 500 °C (2, 6, 12, 24 hours) and 700 °C (24 hours).

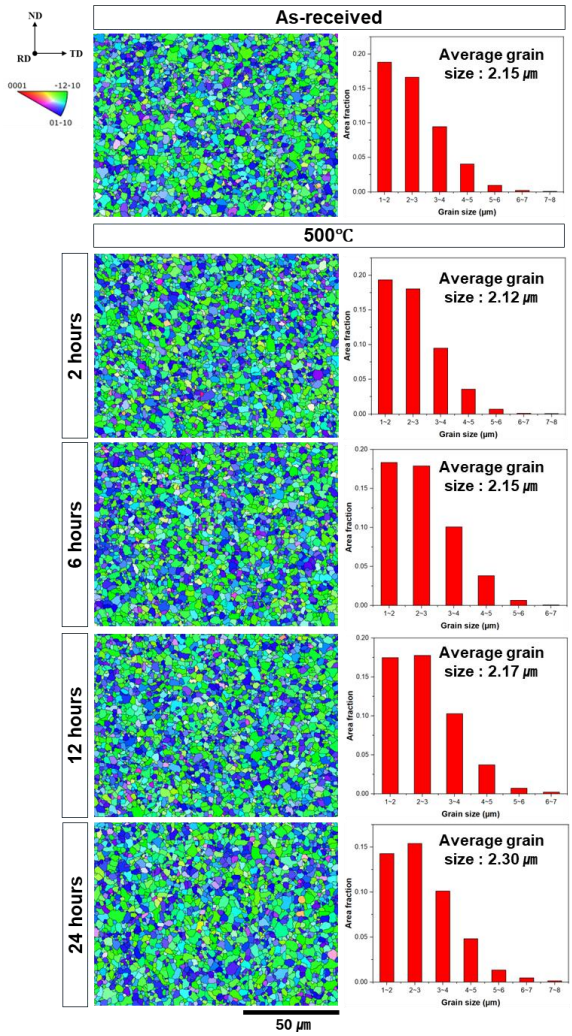

Fig. 2. IPF maps and grain size fraction plots of HANA-6 in the as-received state and after heat treatments at 500 °C for 2, 6, 12, and 24 hours.

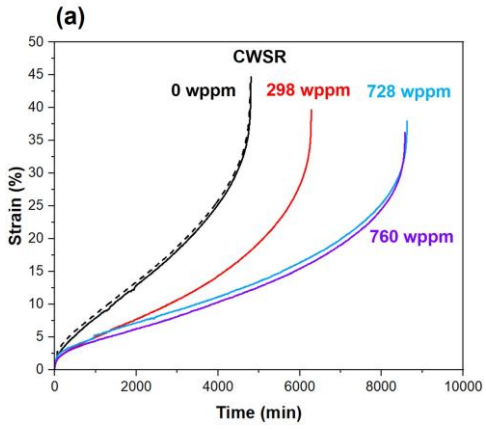

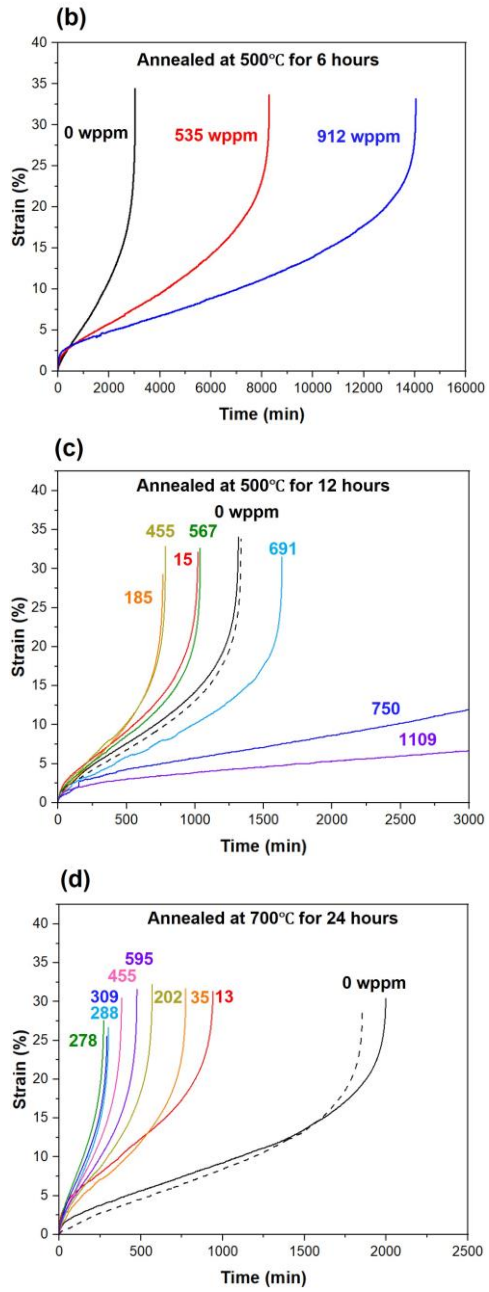

Fig. 3. Creep behavior of Zircaloy-4 at different hydrogen concentrations: (a) cold-worked stress-relieved specimen, (b) recrystallized specimen annealed at 500°C for 6 hours, (c) recrystallized specimen annealed at 500°C for 12 hours, tested at 450°C and 120 MPa, and (d) recrystallized specimen annealed at 700°C for 24 hours, tested at 450°C and 116 MPa.

Figure 4 presents the creep behavior of as-received HANA-6 specimens subjected to different hydrogen contents. Table 4 compiles the values of secondary creep rate, overall strain, and rupture times obtained from these tests. The specimens examined contained hydrogen concentrations ranging between 55 and 755 wppm. The creep response of as-received HANA-6 was comparable to that of Zircaloy-4 that had been heat-treated at 700°C for 24 hours. As the hydrogen content approached the terminal solid solubility for dissolution (TSSD), secondary creep rates increased while rupture times shortened. Once the hydrogen exceeded the TSSD, however, the creep rate declined again, leading to longer rupture times. Across all test conditions, hydrogen-charged specimens fractured earlier than their hydrogen-free counterparts.

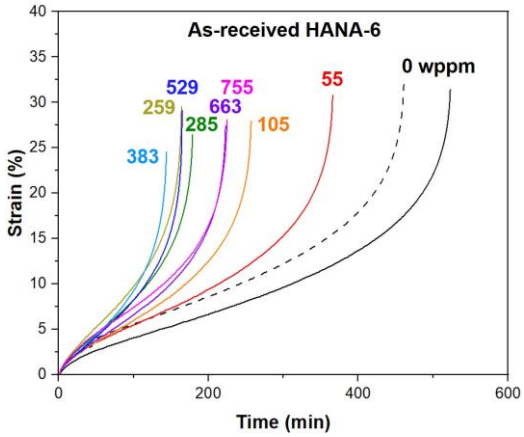

Fig. 4. Creep behavior of HANA-6 at different hydrogen concentrations

3. Conclusions

This study focuses on the effect of hydrogen concentration on the creep behavior of CWSR, RXA, Zircaloy-4, and HANA-6 claddings with various grain sizes.

It is generally recognized that zirconium hydrides exhibit brittle characteristics, leading to a reduction in the tensile strength of cladding as the hydride fraction increases. Nevertheless, in cold-worked stress-relieved (CWSR) cladding, the high defect density promotes the dissolution and migration of hydrogen toward defect sites, thereby inducing localized lattice distortions. Such distortions increase the activation energy required for dislocation motion, resulting in enhanced creep resistance. Consequently, the creep resistance of CWSR cladding improves with increasing hydrogen concentration.

In contrast, the RXA cladding has a lower defect density, allowing hydrogen to be more uniformly distributed while minimizing lattice deformation. This weakens the dislocation movement inhibition effect, lowering the activation energy and promoting deformation. However, when the hydrogen concentration exceeds the TSSD, precipitated hydrides restrict dislocation movement, reducing creep resistance.

In HANA-6 cladding, which has a larger grain size than Zircaloy-4 due to the fabrication process, no significant grain growth was observed even after annealed at 500°C for 24 hours. The creep results for the HANA-6 cladding were similar to those of Zircaloy-4 cladding annealed at 500°C for more than 12 hours. Hydrogen accelerated creep below the TSSD, but

hydrides precipitated after the TSSD increased creep resistance.

These results clearly demonstrated a transition in creep behavior based on the TSSD in specimens with average grain sizes ranging from 1.97 μm (500°C, 6 hours) to 2.6 μm (500°C, 12 hours). This suggests that hydrogen concentration and grain size significantly influence the creep properties of Zircaloy-4.

This study is expected to contribute to the development of standards to ensure the safety and reliability of nuclear fuel cladding by enhancing our understanding of the effects of hydrogen on creep.

ACKNOWLEDGMENTS

REFERENCES

[1] U.S. Nuclear regulatory commission (NRC), Spent Fuel project Office Interim Staff guidance-11, Revision 1, (2000).
[2] U.S. Nuclear regulatory commission (NRC), Spent Fuel project Office Interim Staff guidance-11, Revision 2, (2002).
[3] U.S. Nuclear regulatory commission (NRC), Spent Fuel Project Office Interim Staff Guidance-11, Revision 3, (2003).
[4] J. Stover, NUREG-2216 - Standard Review Plan for Spent Fuel Transportation, Draft Report for Comment.